Apparent Diffusion Coefficient Measurement of Myelofibrosis in Mouse Tibia

version 20230214

I. Executive Summary

The goal of this Co-Clinical Imaging Research Program (CIRP) pre-clinical imaging procedure entitled, "Apparent Diffusion Coefficient Measurement of Myelofibrosis in Mouse Tibia", is to provide detailed description of key steps used to achieve a stated level of performance embodied in "Claims", for MRI measurement of apparent diffusion coefficient (ADC) in tibia bone marrow of myelofibrosis mouse models. This pre-clinical imaging procedure document will be referred to as a "profile" since it has been designed to have some common features with Quantitative Imaging Biomarkers Alliance (QIBA) Profiles targeting standardization of human quantitative imaging procedures (http://qibawiki.rsna.org/index.php/Main_Page).

Myelofibrosis (MF) is a chronic, ultimately fatal myeloproliferative neoplasm caused by genetic mutations in hematopoietic stem cells leading to systemic inflammation and progressive fibrosis disrupting normal architecture and composition of the bone marrow[1, 2]. Bone marrow biopsy, which is painful and subject to sampling error, remains the default method to assess MF disease in humans. The University of Michigan CIRP U24 CA 237683 project involves a longitudinal study design of human MF patients, in parallel with corollary studies of MF mouse models to develop noninvasive quantitative bone marrow MRI methods sensitive to alteration of bone marrow composition due to myelofibrosis evolution and response to MF treatments[3]. The UM CIRP project involves measurement of three image-based metrics (ADC, proton-density fat fraction (PDFF), and magnetization transfer ration (MTR)) that have potential to objectively document MF disease status. Profiles corresponding to PDFF and MTR measurement of MF mouse tibia are also available on the UM CIRP website (UMU24CIRP (umich.edu)) with links to Protocols.io. ADC is known to be sensitive to density of (sub)cellular constituents that impede molecular water mobility [4-6]. This profile details procedures for ADC measurement in MF mouse tibia to achieve stated performance claims.

II. Pre-Clinical Imaging Claims

Tibia bone marrow composition in MF mouse models has gradation going from proximal to distil ends of the tibia, therefore separate claims are made for volume of interest (VOI) analysis of ADC maps for each of three distinct sections along the length of the tibia (see Figure 1):

Section 1 (proximal) ≡ VOI (~4-5mm^3) within 9mm of proximal end of tibia
Section 2 (transition) ≡ VOI (~0.4-0.5mm^3) from 10 to 12mm of proximal end of tibia
Section 3 (distil) ≡ VOI (~0.1-0.2mm^3) from 13 to 14mm of proximal end of tibia

Claim 1: A measured change in the mean ADC in Section 1 VOI of MF mouse model tibia that exceeds ±0.037μm^2/ms indicates a true biological change has occurred in the tibia bone marrow with 95% confidence.

Claim 2: A measured change in the mean ADC in Section 2 VOI of MF mouse model tibia that exceeds ±0.087μm²/ms indicates a true biological change has occurred in the tibia bone marrow with 95% confidence

Claim 3: A measured change in the mean ADC in Section 3 VOI of MF mouse model tibia that exceeds ±0.030μm²/ms indicates a true biological change has occurred in the tibia bone marrow with 95% confidence

The claims hold when:

- **Scanner hardware, diffusion weighted image (DWI) data acquisition method and parameters, image reconstruction, and data-reduction procedures are equivalent (or superior) to those detailed in section III.**
- **Use of the same animal model and interventions to induce myelofibrosis are performed as detailed in section V.**
- **ADC change is assessed on an individual animal basis where each animal undergoes identical procedures on the same MRI system over longitudinal timepoints.**

III. MR Imaging Process Specifications

1. MRI Scanner Hardware
    i. Bruker BioSpec® MRI Console Paravision 7.0.0 software installed on 64 bit Linux multicore workstation, 16 GB RAM, 1TB hard disk.
    ii. 7Tesla, 30cm bore magnet model "7T/310/AS" System (Agilent) with compact Faraday RF-shielding cabinet is attached to the magnet service end
    iii. System gradient/shim coil set model "B-GA12S HP" with standard 300V/200A gradient amplifier and standard 5A shim amplifier:
        a. Inner diameter 114mm
        b. Gradient strength 440 mT/m
        c. Max slew rate 3,440 T/m/s
        d. 10 shim channels, up to 4th order shim coils
    iv. Large Transmit/Receive RF Volume Coil: Outer/inner diameter 112mm/86mm
    v. Medium Transmit/Receive RF Volume Coil: Outer/inner diameter 75mm/40mm RF RES 300 1H 075/040 QSN TR; model 1P T13161V3.
    vi. Small Receive: CryoProbe™ 4 Element Array RF Coil Kit for Mice cryogenically cooled to 20-30°K with parallel receiver upgrade.

2. Acquisition Technique
    i. Single spin-echo, 3-orthogonal diffusion weighted axes, non echo-planar imaging. Sequence "Method=<Bruker:DtiStandard>"

ii. 2D multi-slice in coronal plane with geometry:

Table I: DWI geometry

Matrix	Acquired Voxel Size (μm)	FOV (mm)
128 (freq enc on z-axis)	180 on z	23.04 on z
64 (phase enc on x-axis	150 on x	9.6 on x
40 (slices, y-axis)	150 (slice thickness) on y	6.0 on y

iii. Contrast Control: TR/TE=2000/22ms; spectral fat-suppression; 2 NSA; b-values = 0 and 3000s/mm^2 on each of three orthogonal axes (X,Y,Z); diffusion pulse timing δ = 4ms, Δ = 10ms; DWI series scan time = 17min.
iv. Conventional 2D sequential cartesian k-space trajectory, 1 phase-encode / TR.
v. Full k-space acquisition, no acceleration, no multi-band, no turbo spin-echo.
vi. No physiologic synchronization. Anesthetized mouse leg is held in place between 3D-printed, leg-shaped mold on posterior side and CryoProbe™ on anterior side.

3. Image Reconstruction
   i. Time-domain DWI are reconstructed to magnitude space-domain images on the Bruker system console using standard 2DFT image reconstruction routines within the Paravision 7.0.0 environment. Directional diffusion-weighted images for nominal b=0, and b=3000 along X, Y, Z directions are reconstructed separately and stored on disk within standard Bruker "pdata" data tree in "2dseq" datafile, a native Bruker format. Associated Bruker-generated text files "acqp", "AdjStatePerScan", "configscan", "method", "pulseprogram", "specpar", "id", "methreco", "procs", "reco", and "visu_pars" are stored in series-level folders within the exam-level folder. Exam-level folders, coded by group+mouseID+acqdate+acqtime are transferred to university-maintained drives for archival and subsequent analysis described below.

4. Biomarker Map Generation
   i. Conversion from Bruker 2dseq-format DWI to ITK-compatible format is performed using a custom MATLAB (ver ≥2016b) "ProcessLegTLC.m" script that relies on scripts within Bruker-provided "pvmatlab" (ver 2013) MATLAB package for handling ParaVision data.
   ii. Initially, ProcessLegTLC script surveys all "method" text files for parameter values of keywords to create a catalog of the entire exam. The catalog is stored in a "GroupID_MouseID_DateTime_Catalog.tsv" text file containing key attributes for each series: [Series#; ScanTime; Protocol; Method; TR; TE; NEcho; Nave; PVM_Matrix; Thk; Nslc; MTsatFreq; MTstate; Receiver_Gain; ReconSize; bvalue].
   iii. Subsequent processing within ProcessLegTLC loads DWI 2dseq data into 4-dimensional arrays for calculation of ADC maps using directional b-values extracted from the Bruker acqp text file. Geometry content (slice location, extent and angulation) is fully retained.

iv. ADC maps were derived for pixels having signal > 0.2 x Mean signal of trace diffusion weighted image (*DWI$_{trace}$*) as well as DWI$_{b0}$/DWI$_{highb}$ ≥ 1 to reject unreliable pixels in ADC maps. Then *DWI$_{trace}$* and *ADC* maps are calculated using each *jth* directional b-value, then averaged into an isotropic *ADC*:

$$ADC_j = \frac{1}{b_j}\, ln\left[\frac{DWI_{b0}}{DWI_{b_j}}\right];\ \ ADC = [ADC_X + ADC_Y + ADC_Z]/3$$

$$DWI_{trace} = \sqrt[\frac{1}{3}]{[DWI_{b_X} \cdot DWI_{b_Y} \cdot DWI_{b_Z}]};$$

v. *DWI$_{b0}$*, *DWI$_{trace}$*, and *ADC* map are stored on disk in ITK-compatible MetaImage format [7] comprised of paired header (eg. "ABCD.mhd") and binary data (eg. "ABCD.raw") 3D volumes for compactness and portability to commonly used medical/scientific image viewing platforms, such as ITK-SNAP and 3DSlicer [8]. Geometry content are accurately reflected in the mhd header. ADC maps are scaled so pixel values are in (μm^2/ms) units; e.g. ADC$_{muscle}$ ≈ 0.8 μm^2/ms.

5. Additional Map Conditioning

Data reported in this profile *DID NOT* undergo additional conditioning beyond that detailed in sections 6 through 9 below. However, spatial registration of image volumes will be performed in UM CIRP U24 CA 237683 study of MF in mouse tibia to longitudinally follow disease evolution and response to treatment. For completeness, the process for spatial registration of a mouse tibia over time is described below:

i. MATLAB scripts with a GUI interface were developed in the UM Center for Molecular Imaging (CMI) to facilitate MATLAB calls to Elastix (ver 4.8) image registration software (elastix: download (lumc.nl)). This tool was designed to input/output MetaImage format 3D volumes as created by ProcessLegTLC script.

ii. In addition to multi-slice *ADC*, *DWI$_{b=0}$* and *DWI$_{b=3000}$*, the MF tibia MRI protocol includes a variety of imaging contrasts including: multi-echo 3D gradient-echo for proton-density fat-fraction (PDFF); magnetization-transfer (MT) RF pulses "OFF" and "ON" for calculation of magnetization transfer ratio (MTR). The 3D MTOFF is used as the reference "FIXED" image volume to which the *DWI$_{b=0}$* image volume, here called "MOVER", is transformed to spatially align with the FIXED volume.

iii. The tibia is effectively a rigid body, whereas surrounding muscle may be deformed over serial MRI sessions. Therefore, the tibia is manually segmented on the FIXED image baseline timepoint using the CMI GUI (or 3DSlicer) and saved in MetaImage format. A dilated version of the tibia VOI segmentation serves as a mask to drive the Elastix rigid-body volume registration routine based on tibia anatomic features without regard to muscle features.

iv. The CMI GUI prompts user to identify 4 points on the FIXED tibia along with 4 homologous points on the MOVER tibia to initialize the Euler (rigid body) transformation. For this step, two landmarks on the distil end of the tibia and two mid-tibia are used.

v. Main Elastix parameters are:

a. FIXED = "*_MT_Off.mhd"
b. MOVER = "*_DWI_T2w.mhd" (is DWIb=0)
c. MASK = "*_MT_Off_VOI.mhd"
d. Sample: RandomSparseMask
e. Metric: Mutual Information
f. Transform: Euler
g. Final Interpolation: BSpline-3
h. Iterations: 4000
i. NSamples: 5000

vi. Complete Elastix parameter file is provided in Appendix I.
Since $DWI_{b=0}$, $DWI_{b=3000}$, and *ADC* maps have identical acquisition geometry, the final spatial transformation that aligns $DWI_{b=0}$ (mover) to fixed reference is applied to $DWI_{b=3000}$, and *ADC*. All spatially registered volumes are output to disk with their original filename amended by an "_R". Elastixlog.txt, ElastixParameters.txt, and TransformParamters.txt are also retained in sub-folders for future use.

6. Region / Volume of Interest (ROI / VOI) Segmentation
   i. For longitudinal datasets spatially-registered to common (FIXED) dataset, the original tibia segmentation saved in "*_MT_Off_VOI.mhd" may be applied to any co-registered datasets. This *WAS NOT DONE* nor was it necessary for data, analysis and results reported in this profile.
   ii. For this profile reporting repeatability ADC measurement in MF mouse tibia using test-retest design, the tibia was manually segmented independently for each Test and ReTest dataset. Also note, the CMI GUI or other 3D image analysis platform such as 3DSlicer may be used to manually segment tibia with the resultant output stored in MetaImage format [7] with "*_VOI.mhd" filename. For this profile, both Test and ReTest datasets from all mice and timepoints were manually segmented using the CMI GUI by one individual (KH).
   iii. Apparent gradation of ADC from proximal to distil ends of the tibia was dealt with by separate analysis of three sections along the length of the tibia with separate repeatability claims.
   iv. To systematically define these sections, a dedicated MATLAB script was created to read-in the ADC and VOI mask and automatically detect a landmark (knee) defined as the Z-slice containing largest VOI cross-section in X-Y plane. Then given known slice thickness, three sections were parsed by Z-dimension from the VOI as displayed in Figure 1.

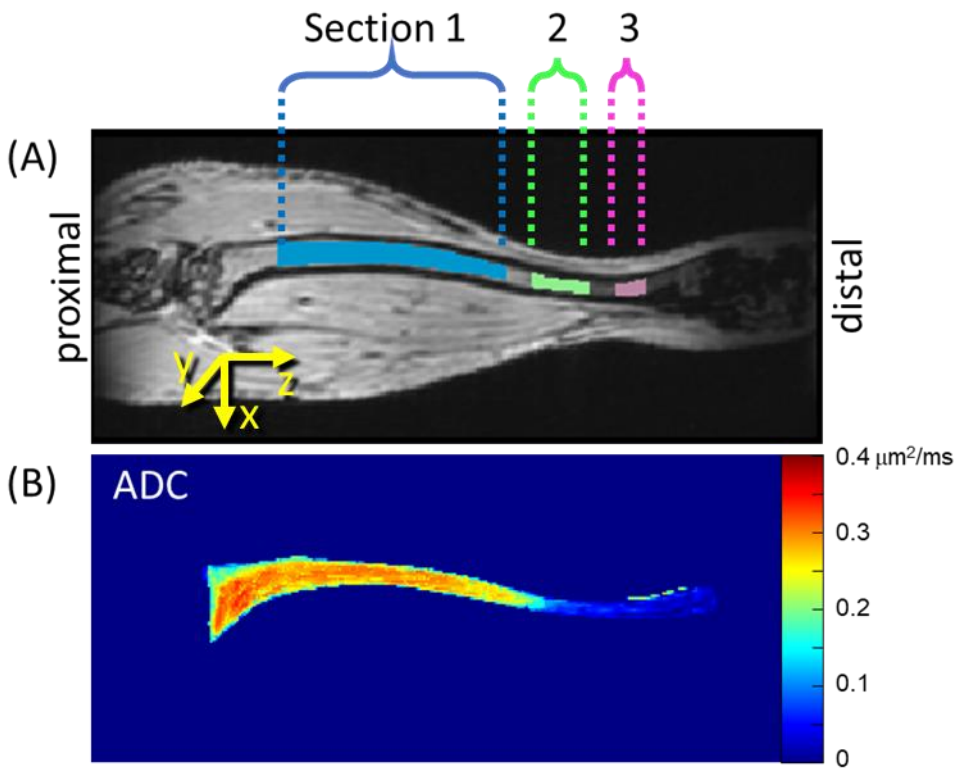

Figure 1: (A) Coronal slice through volumes of interest (VOI) along length of tibia relative to reference point determined by greatest axial tibia area assigned location "z=0mm". Relative to this reference, Section 1 spans z = 1.8 to 9mm, Section 2 z = 9.8 to 11.7mm, and Section 3 z = 12.6 to 13.5mm for all mice. (B) Coronal projection of mean ADC value within the tibia in $\mu m^2/ms$ units.

7. Biomarker Metric
    i. Three-D masks for Sections 1,2,3 were applied independently to ADC maps to extract mean ADC of voxels in each section, which is taken as the "biomarker". Repeatability of mean ADC for each section was analyzed by test-retest study design where MF model mice were scanned on two consecutive days where biological change in the tibia over 1 day is assumed to be small/insignificant relative to MF disease that develops over several weeks to month interval.

8. Imaging System Performance Validation
    i. An ice-water design DWI phantom was used to provide temperature control for an absolute diffusion coefficient reference standard = $1.1 \mu m^2/ms$.
    ii. This phantom is the same as used in the "DWI Phantom Round Robin" conducted by the CIRP Image Acquisition and Data Processing (IADP) work group. Details of the phantom design, preparation, and scanning procedure are provided in *UMU24CIRP - SOP Directory (umich.edu)*.

iii. Due to DWI phantom size, the CryoProbe™ 4 element receiver RF coil could not be used. Instead, the 40mm ID transmit/receive volume RF coil was used at the expense of lower SNR relative to the CryoProbe™.

iv. Referring to Figure 2, absolute ADC bias is less than 1% at magnet isocenter of the Bruker 7T MRI system, and RMSE relative to truth (1.1µm²/ms) is ~3% over the central 38mm length along Z-axis. This level of accuracy and spatial uniformity should be adequate for serial ADC measurements on MF mouse tibia which is approximately 17mm long.

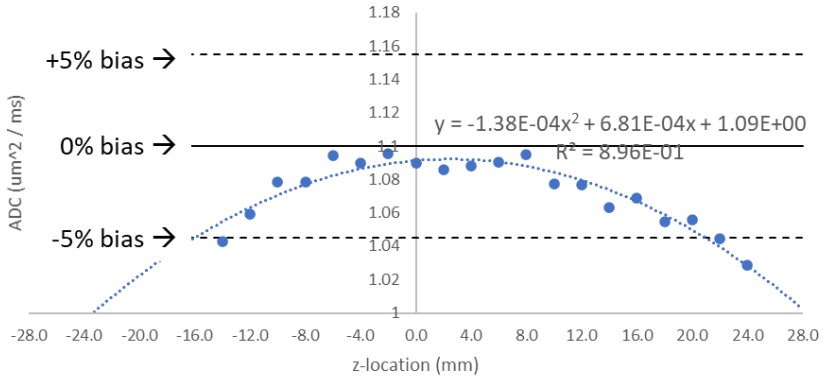

Figure 2: Absolute bias and spatial uniformity of ADC measurements on UM Bruker 7T system determined by ice-water DWI phantom.

IV. Quantitative Metrics, Statistical Methods and Data Supporting Claim(s)

i. Repeatability of VOI mean ADC in MF mouse tibia was assessed using a "test-retest" design study [9, 10].

ii. A total of 15 female BALB/c JAK2 mutant MF model mice were included in this study. MF disease model was induced by whole body irradiation to ablate bone marrow, followed by same day bone-marrow transplant (BMT) a 50% - 50% combination of normal and diseased cells per the protocol summarized in Section IV below. DWI was acquired over 4 to 10 weeks following BMT as the disease developed in the marrow space. Each test-retest DWI dataset pair was acquired on two consecutive days for each animal, followed by 9 to 14 days without DWI. Typically, test-retest pairs were spaced 10 to 14 days apart, such that a total of 33 test-retest pairs were collected from these 15 mice. Since the disease develops relatively slowly over the 10 weeks following BMT, the biological status of bone marrow over any given 24 hour period (i.e. a test-retest pair) is assumed to be effectively constant. Moreover, while correlation between pairs from a given animal is possible, the 33 test-retest pairs were treated as independent measurements to simplify test-retest analysis.

iii. DWI targets water mobility, though residual unsuppressed fat signal in normal and MF diseased marrow can complicate ADC quantification since fat has an extremely low diffusion coefficient. Spectral fat suppression RF pulses were used, although fat suppression may be incomplete where local B0 shimming is suboptimal which tends to happen toward the distil end of the tibia (Section 2 and 3). To limit inclusion of fat-dominated ADC data in the analysis, a test-retest pair was excluded if on either test or retest dataset the mean ADC VOIs

was < 0.05μm^2/ms. This filter meant number of usable test-retest pairs was lower in Sections 2 and 3 relative to Section 1.

iv. Explicit steps to assess repeatability followed Bland-Altman and QIBA-recommended procedures summarized as [9-11]:

a. Calculate mean (M) and variance (V) for each test-retest pair

$$M = \frac{(MeanADC_{test} + MeanADC_{retest})}{2};\ V = \frac{(MeanADC_{test} - MeanADC_{retest})^2}{2}$$

b. For each of N-pairs, calculate V/(M^2), take the mean over all N-pairs, then take square root to get within-subject coefficient of variation, wCV (in % units):

$$wCV = 100\% \cdot \sqrt{\frac{1}{N}\sum_i^N \frac{V_i}{M_i^2}}$$

c. Note, wCV is a relative (dimensionless) repeatability metric. For non-relative repeatability in ADC units (μm^2/ms), use within-subject standard deviation, wSD, and repeatability coefficient, RC given by:

$$wSD = \sqrt{\frac{1}{N}\sum_i^N V_i}$$
$$RC = 2.77 \cdot wSD$$

d. The RC is a measure of precision and useful to infer minimum threshold of observed biomarker change attributable to true biologic change (with 95% confidence), as opposed to measurement error.

e. The corresponding 95% confidence interval (α = 0.05) to RC are given by multiplicative lower-bound (LB) and upper-bound (UB) factors given by ChiSqr function for N-1 degrees of freedom [9, 10]:

$$95\%\ CI\ of\ RC = RC \cdot \left[\frac{1}{\sqrt{(N-1)\cdot\ \chi^2_{0.975}}};\ \frac{1}{\sqrt{(N-1)\cdot\ \chi^2_{0.025}}}\right]$$

f. The same multiplicative factors were used to estimate 95% CI's for wCV and wSD indicated by [lower bound (LB), upper bound (UB)]. Test-retest results are summarized in Table II:

Table II	Section 1	Section 2	Section 3
N Test-Retest Pairs	33	29	20
Mean ADC (μm^2/ms)	0.317	0.175	0.069
Bias (ADCretest – ADCtest) (μm^2/ms)	0.008	0.015	0.009
wCV [LB, UB] (%)	4.4 [3.5, 5.8]	21.9 [17.4, 29.6]	15.0 [11.4, 21.9]
wSD [LB, UB] (μm^2/ms)	0.013 [0.011, 0.018]	0.031 [0.025, 0.042]	0.011 [0.008, 0.016]
RC [LB, UB] (μm^2/ms)	0.037 [0.031, 0.05]	0.087 [0.069, 0.116]	0.030 [0.022, 0.044]

g. Bland-Altman x-y plots provide a graphic view of repeatability [11], where x = (ADC_{retest} + ADC_{test})/2 and y = (ADC_{retest} - ADC_{test}). Mean of y is a measure of bias (dotted line), or apparent ADC change between test and retest conditions. Ideally, bias is close to zero thereby supporting the assumption that bone marrow was biologically constant between test and retest measurements. Dashed lines (bias ± 1.96*std(ADC_{retest} - ADC_{test})) provide a graphical indication of measurement precision. Slight positive bias over the 1-day test-retest interval is consistent with significant overall ADC increase over 8weeks as the disease developed.

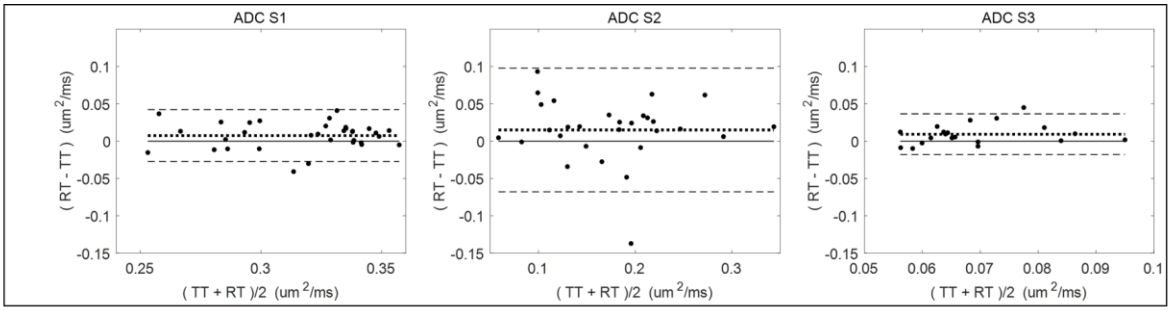

Figure 2: Bland-Altman plots graphically illustrate biomarker repeatability between Test (TT) and Retest (RT) paired measurements for ADC. Plots for Sections S1, S2, and S3 are in left, center, right panels, respectively. Mean difference (RT–TT) shown as dotted lines, and dashed lines represent confidence range defined as mean difference ± 1.96 * std(RT-TT). Vertical scale is held constant for each given biomarker to illustrate repeatability dependence on section (see Figure 1). Refer to Table 2 for number of TT, RT-pairs in each plot.

V. Animal Model Specifications

1. Species: mouse
2. Strain: C57BL/6 purchased from Charles River Laboratories (Wilmington, MA).
3. Sex: Female
4. Disease induction: The JAK2 V617F (Jak2+/VF) animal model of myelofibrosis (MF) was generated using resultant 8-10 week old female donor offspring from a cross between Jak2+/Fl mice (B6N.129S6(SJL)-Jak2tm1.2Ble/AmlyJ; Jackson Laboratory Stock No. 031658) and Mx-Cre mice (B6.Cg-Tg(Mx1-cre)1Cgn/J; Jackson Laboratory Stock No. 003556), similar to previously described methods [9, 20]. Briefly, whole bone marrow cells were isolated from donor mice, and mixed 1:1 with whole bone marrow cells isolated from age- and gender-matched wild-type C57Bl/6 mice. A total of 1 x 107 mixed bone marrow cells was injected retro-orbitally into lethally irradiated 6 week old female recipient C57Bl/6 mice. Polyinosinic-polycytidylic acid (10 mg/kg) was administered intra-peritoneally 10 days post-bone marrow transplant (post-BMT) for induction of Cre recombinase-mediated replacement of the floxed endogenous exon with the mutated exon of Jak2 for expression of the JAK2 V617F mutant allele.
5. Therapeutic intervention – Not Applicable.
6. Animal age at start of MRI data acquisition: ~12 weeks (approximately 28 days post- BMT).
7. Animal prep and during imaging: 1.5% Isofluorane/air inhalation.
8. Animal monitoring/support during imaging:
    i. Thermoregulated heating bed during imaging (37^{o}C)
    ii. Respiratory montoring (SAI monitor)
9. Animal recovery: isolated cage until full recovery, then back to communal cage
10. Imaging schedule: Each test-retest DWI dataset pair was acquired on two consecutive days for each animal starting ~28 days post-BMT. Additional test-retest pairs were spaced approximately 10 to 14 days apart, such that a total of 33 test-retest pairs were collected from 15 mice.
11. UM Laboratory Animal Medicine Approval Code: #PRO00010851 and date: 09/26/22.

VI. Outcome Specifications

1. Time to moribund/survival
2. Longitudinal body weight and spleen volume measurements (last MRI) and spleen weight at sacrifice
3. Tibia and spleen tissues were harvested for flow cytometry and histological analysis
    i. Complete Blood Count (CBC); flow cytometry for immune cell populations
    ii. Liver and spleen weight
    iii. Liver, spleen and femur/tibia histology preparation and staining
    iv. Immune cell populations of spleen and bone marrow
    v. Immuno-blotting of spleen tissue

References

1. Garmezy, B., et al., *A provider's guide to primary myelofibrosis: pathophysiology, diagnosis, and management.* Blood Rev, 2021. **45**: p. 100691.
2. Schaefer, J.K., et al., *Primary myelofibrosis evolving to an aplastic appearing marrow.* Clin Case Rep, 2018. **6**(7): p. 1393-1395.
3. Luker, G.D., et al., *A Pilot Study of Quantitative MRI Parametric Response Mapping of Bone Marrow Fat for Treatment Assessment in Myelofibrosis.* Tomography, 2016. **2**(1): p. 67-78.
4. Meyer, H.J., A. Wienke, and A. Surov, *ADC values of benign and high grade meningiomas and associations with tumor cellularity and proliferation - A systematic review and meta-analysis.* J Neurol Sci, 2020. **415**: p. 116975.
5. Padhani, A.R., et al., *Diffusion-weighted magnetic resonance imaging as a cancer biomarker: consensus and recommendations.* Neoplasia, 2009. **11**(2): p. 102-25.
6. Sorace, A.G., et al., *Imaging for Response Assessment in Cancer Clinical Trials.* Semin Nucl Med, 2020. **50**(6): p. 488-504.
7. *Metaimage MHD Format*. Available from: https://itk.org/Wiki/ITK/MetaIO/Documentation#:~:text=MetaImage%20is%20the%20text%2Dbased,library%20is%20known%20at%20MetaIO.
8. *3D Slicer*. Available from: https://www.slicer.org/#what-is-3d-slicer.
9. Raunig, D.L., et al., *Quantitative imaging biomarkers: a review of statistical methods for technical performance assessment.* Stat Methods Med Res, 2015. **24**(1): p. 27-67.
10. Winfield, J.M., et al., *Extracranial Soft-Tissue Tumors: Repeatability of Apparent Diffusion Coefficient Estimates from Diffusion-weighted MR Imaging.* Radiology, 2017. **284**(1): p. 88-99.
11. Bland, J.M. and D.G. Altman, *Statistical methods for assessing agreement between two methods of clinical measurement.* Lancet, 1986. **1**(8476): p. 307-10.

Appendix I: Elastix Parameters (automatically retained in “ElastixParameters.txt” file)

```
(FixedInternalImagePixelType "float")
(FixedImageDimension  3)
(MovingInternalImagePixelType "float")
(MovingImagedimension  3)
(UseDirectionCosines "false")
(WriteTransformParametersEachIteration "false")
(WriteTransformParametersEachResolution "true")
(WriteResultImageAfterEachResolution "false")
(WriteResultImage "true")
(Registration "MultiResolutionRegistration")
(Metric "AdvancedMattesMutualInformation")
(UseJacobianPreconditioning "false")
(FiniteDifferenceDerivative "false")
(ShowExactMetricValue "false")
(UseFastAndLowMemoryVersion "false")
(NumberOfHistogramBins  32)
(NumberOfFixedHistogramBins  32)
(NumberOfMovingHistogramBins  32)
(FixedLimitRangeRatio  0)
(MovingLimitRangeRatio  0)
(FixedKernelBSplineOrder  1)
(MovingKernelBSplineOrder  3)
(ImageSampler "RandomSparseMask")
(NumberOfSpatialSamples  5000)
(NewSamplesEveryIteration "true")
(UseRandomSampleRegion "false")
(CheckNumberOfSamples "true")
(Interpolator "LinearInterpolator")
(ResampleInterpolator "FinalBSplineInterpolator")
(FinalBSplineInterpolationOrder  3)
(Resampler "DefaultResampler")
(ResultImageFormat "mhd")
(ResultImagePixelType "float")
(ErodeFixedMask "false")
(ErodeMovingMask "false")
(DefaultPixelValue  0)
(Transform "EulerTransform")
(AutomaticTransformInitialization "false")
(AutomaticScalesEstimation "true")
(HowToCombineTransforms "Compose")
(Optimizer "StandardGradientDescent")
```

```
(NumberOfSamplesForSelfHessian 100000)
(NumberOfGradientMeasurements 0)
(NumberOfJacobianMeasurements 2700)
(NumberOfSamplesForExactGradient 100000)
(MaximumNumberOfIterations 4000)
(MaximumNumberOfSamplingAttempts 0)
(SP_a 2)
(SP_alpha 0.60200000)
(SP_A 50)
(NumberOfResolutions 1)
(FixedImagePyramid "FixedSmoothingImagePyramid")
(FixedImagePyramidSchedule 1 1 1)
(MovingImagePyramid "MovingSmoothingImagePyramid")
(MovingImagePyramidSchedule 1 1 1)
(Scales 10000 10000 10000 1 1 1)
```